

## Dielectric response of N<sub>2</sub>-Ar solid solutions in the audio frequency range

S. Pilla,\* J. A. Hamida, K. A. Muttalib, and N. S. Sullivan

Department of Physics, University of Florida, Gainesville, Florida 32611

(Received 9 January 2002; revised manuscript received 12 February 2003; published 23 May 2003)

High sensitivity dielectric measurements are reported for N<sub>2</sub>-Ar solid mixtures for 49 <  $x(\text{N}_2)$  < 100 mol%. The results show the onset of strong hysteresis effects for the temperature dependence of the dielectric constant on thermal cycling below 30 K. These onset temperatures are identified with transitions to a quadrupolar glass state. Samples cooled from high temperatures (above 50 K) in the presence of a small external ac electric field also show a characteristic field-cooled history dependence down to 50% dilution of N<sub>2</sub>. The results presented are purely empirical, but qualitative estimates of the magnitude of the effects using a generalized fluctuation-dissipation argument are consistent with the observations.

DOI: 10.1103/PhysRevB.67.174204

PACS number(s): 64.60.Cn, 77.22.-d

### I. OVERVIEW

While ordinary glasses represent one of the oldest materials known to man, a comprehensive understanding of the formation of glasses has not yet been achieved. For this reason, interest has become focused on conceptually simpler systems that can serve as prototypes for studying the underlying physics of glasses in general. The study of the so-called spin glasses has shown that the interplay between frustration and disorder<sup>1</sup> plays a key role in determining the glasslike properties of these compounds. Dilute systems of interacting quadrupoles, such as ortho-para H<sub>2</sub>, ortho-para D<sub>2</sub>, N<sub>2</sub>-Ar mixtures, and KCN-KBr solid solutions, which incorporate in a simple way both frustration and disorder, have therefore received a growing interest for studying glass formation. The frustration in these systems is geometrical in nature because it arises from the topological impossibility of ensuring the minimum possible energy for all pairs of neighboring electric quadrupoles, and disorder comes from site replacement of some of the quadrupole bearing molecules by noninteracting atoms. These molecular solids are therefore members of a new class of systems exhibiting strong geometrical frustration for which phenomena have been recently observed for the magnetic analogs.<sup>2,3</sup> In the case of N<sub>2</sub>-Ar solid solutions, the oblate spheroid shaped N<sub>2</sub> molecules bear electric quadrupole moments while spherical noninteracting Ar atoms play the role of disorder. The interactions between N<sub>2</sub> molecules are short ranged and well characterized, and due to the large physical sizes of the molecules the system can be treated classically. The effect of disorder can be systematically studied in this system by changing the Ar concentration. For N<sub>2</sub> concentrations greater than about 80%, the N<sub>2</sub> molecules achieve a long-range orientational order at low temperatures despite frustration and disorder. However, this ordering occurs only following a structural transition from the high temperature hcp lattice to a low temperature ( $T < 35.6$  K) fcc lattice, and results in a periodic Pa3 structure<sup>4</sup> for the quadrupoles. The structural and the orientational order-disorder transitions appear to occur along the same phase boundary for high N<sub>2</sub> concentrations.

At much lower N<sub>2</sub> concentrations (<55%), there exists a reentrant transition to the fcc lattice (Fig. 1). It has been proposed that this transition is also accompanied by the

appearance of a quasi-long-range quadrupolar ordered phase (phase IB).<sup>5,6</sup> At intermediate N<sub>2</sub> concentrations, 57 <  $x(\text{N}_2)$  < 78 mol%, the lattice symmetry remains hcp and NMR studies show that for this lattice structure, the low-temperature state is glasslike with random orientations for the molecular axes and a broad range of values for the local order parameters. The local orientational ordering is specified by two sets of parameters (i) the local orthonormal axes ( $x_i, y_i, z_i$ ) associated with the mean orientation of the internuclear axis of each molecule  $i$  and (ii) the intrinsic quadrupolar parameters given by the mean alignment  $\sigma_i = \langle 2z_i^2 - (x_i^2 + y_i^2) \rangle$  and mean eccentricity  $\eta_i = \langle x_i^2 - y_i^2 \rangle$  with respect to these local axes. In terms of the polar angles ( $\theta_i, \phi_i$ ) that specify the instantaneous alignment of the molecule with respect to these mean axes  $\sigma_i = \langle (3 \cos^2 \theta_i$

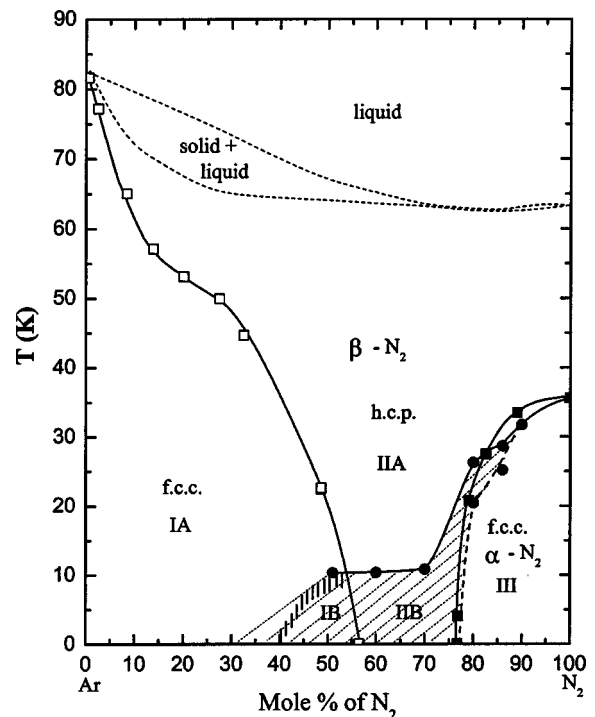


FIG. 1. N<sub>2</sub>-Ar phase diagram showing the glass-phase boundary deduced from the dielectric response of these solid solutions discussed in Sec. II.

$-1/2\rangle$  and  $\eta_i = \langle 2 \sin^2 \theta_i \cos 2\phi_i \rangle$ . The short range correlations between the axes and the order parameters distinguishes the glass state from the independent particle paraelectric state. The temperature dependence of the local order parameters observed by the NMR measurements was smooth with no clear abrupt transition temperature or evidence for the expected hysteresis or nonequilibrium behavior expected for a glass state. Analysis of the NMR experiments also showed that at low temperatures the glass states were characterized by a broad distribution of order parameters, and this property and the general temperature dependence has been verified by recent computer simulations.<sup>1,7</sup>

The purpose of the experiments reported here was to study the dielectric response function using high sensitivity methods to test for the existence of the characteristic glass features in solid  $N_2$ -Ar mixtures where, because of the high polarizability of the  $N_2$  molecules (compared, for example, to  $H_2$ ), one would have much higher sensitivities for probing the glasslike features than in the NMR experiments. The experiments were stimulated by the striking field-cooling effects observed recently in the electric susceptibility measurements of solid  $N_2$ .<sup>8-10</sup> When field-cooled from high temperature in the presence of a small ac electric excitation field, pure  $N_2$  showed distinct memory and aging effects even on cooling into the low temperature fcc phase. This electric field induced behavior occurs without the presence of disorder and is believed to result from the complex geometrical nature of the frustration of the interactions and steric hindrance that lead to a significant coupling of the center-of-mass positions of the molecules and the relative orientations of the molecular axes. These memory effects are not expected for the pure systems where glass states are not observed, and they persist even after very careful annealing procedures, showing that they are not generated by common coarse-grained defect formation (cracks, bubbles, impurities, etc.). It is, however, possible that the behavior is linked to the crystalline martensitic lattice changes, hcp-to-fcc transitions, that accompany the orientational ordering transitions in these systems.<sup>11</sup> It has been postulated<sup>11</sup> that these Martensitic transitions generate memory effects in which skeletal threads of the hcp grain boundaries remain in the ordered fcc structure after the transitions. These persistent defect areas can then nucleate areas of high dielectric polarization in the presence of applied electric fields, which will in turn result in induced anisotropy for the dielectric susceptibility. Similar to the phenomena observed for magnetic spin glasses and other frustrated magnetic systems,<sup>12</sup> relatively small applied fields can then be used to demonstrate memory effects. In particular, the results observed for the molecular glasses should show similarities to the aging and memory effects observed for the dynamic susceptibility of the magnetic spin glasses CuMn and CdCr<sub>1.7</sub>In<sub>0.3</sub>S<sub>4</sub>.<sup>13</sup>

## II. PHASE DIAGRAM

The first structural phase diagram for  $(N_2)_x$ -Ar<sub>1-x</sub> solid mixtures was reported by Barrett and Meyer using x-ray diffraction.<sup>14</sup> The phase diagram is shown in Fig. 1 with the solid lines and solid squares designating the observed transi-

tion temperatures for the abrupt lattice changes from the hcp phase (region II) to the fcc phase (region III). No structural transition was observed for  $56\% < x(N_2) < 77\%$ , and no periodic long range orientational ordering was detected in the entire hcp phase down to 2 K. <sup>15</sup> NMR measurements of <sup>15</sup>N<sub>2</sub> in N<sub>2</sub>-Ar mixtures revealed a quadrupolar glass state<sup>16</sup> below 10 K for  $x(N_2) = 67\%$ . In this glass state, both the principal axes for the molecular quadrupoles and the local order parameters evaluated with respect to those axes vary at random throughout the sample. Furthermore, the values of the order parameters were observed to be frozen with respect to temperature below about 6 K with the low temperature limits considerably less than the rigid orientation values  $\sigma_i = 1, \eta_i = 0$ . (The NMR line shapes are very different if only the molecular axes are random. The state with both axes and order parameters varying at random has been referred to as a quadrupolar glass to distinguish that state from an orientational glass in which only the orientations of the axes occur at random.) Only quadrupolar or orientational glass states have been reported as long as the lattice structure is hcp.<sup>1,5,6,14-25</sup> No slow rotations were detected using spin echoes and stimulated echo techniques<sup>16</sup> in this regime. Neutron scattering on samples with  $x(N_2) = 72\%$  observed only short range orientational order at low temperatures.<sup>20</sup> The disorder was found to be dynamic at high temperatures and “frozen-in” at lower temperatures. Specific heat measurements at these concentrations<sup>19</sup> did not show any discontinuous behavior, or slow thermal relaxations, that occur in ordinary glasses. It was not clear from these studies if the absence of relaxation effects was due to the time scale of observation or whether the effects were too small to be detected by the NMR and thermodynamic measurements.

While much scattered information is available from all these experiments, no systematic measurements have been carried out to map out the orientational and quadrupolar phase boundaries as a function of  $N_2$  concentration. In particular, for  $N_2$  concentrations close to 50%, Hamida *et al.*<sup>5,6</sup> have deduced the existence of a quasi-long-range quadrupolar ordered state in the reentrant fcc structure based on the observation of a very sharp distribution of the quadrupolar order parameters observed by NMR. In this quadrupolar state (region IB in Fig. 1), the molecular axes may either be ordered periodically or distributed at random, but the mean order parameters evaluated with respect to those local axes have a very narrow distribution. This is distinct from the neighboring quadrupolar glass phase (region IIB) with approximately the same substitutional disorder but in the hcp phase. The NMR experiments carried out for powder samples measure only the local (quadrupolar) order parameter distribution and do not provide information about the ordering of the axes. It is therefore not known whether the quadrupolar ordering that reappears in the fcc structure is due to the lowering of frustration or another effect. In the present work, we report systematic studies of the ac dielectric constant for a wide range of  $N_2$  concentrations that were carried out to obtain more precise information about the orientational ordering near the glass transition regions, and to test for the hysteresis and aging effects that characterize glass behavior.

Dielectric spectroscopy can be used to determine the molecular reorientation rates in polar and nonpolar systems. The anisotropic component of the dielectric susceptibility of an ensemble of nonpolar molecules is directly related to the local order parameters. The polarizability  $\alpha$  is separable into an isotropic component  $\alpha_{\text{iso}}$  and an anisotropic component  $\alpha_{\text{aniso}}$ . The average polarizability is defined as  $\alpha_0 = \frac{1}{3}(\alpha_{\parallel} + 2\alpha_{\perp})$  where  $\alpha_{\parallel}$  and  $\alpha_{\perp}$  are the polarizabilities parallel and perpendicular to the molecular axes, respectively. The isotropic component is simply  $\alpha_{\perp}$  and the anisotropic component is given by<sup>9,26,27</sup>

$$\alpha_{\text{aniso}} = \frac{1}{3} \Delta \alpha \langle \langle 3 \cos^2 \theta_E(i) - 1 \rangle \rangle, \quad (1)$$

where  $\Delta \alpha = (\alpha_{\parallel} - \alpha_{\perp})$ .  $\theta_E(i)$  is the polar angle specifying the orientation of the applied electric field with respect to the instantaneous molecular axes  $(x_i, y_i, z_i)$  of the  $i$ th molecule. The average  $\langle \langle \dots \rangle \rangle$  refers to both a configurational and a time average. The anisotropy is very high for N<sub>2</sub> molecules  $\Delta \alpha / \alpha_0 = 0.4$ , (Ref. 28) and as a consequence, dielectric measurements can provide a powerful tool for probing the glass formation over a range of frequencies that are especially relevant to the dynamical time scale of the glass freezing in this system. The polarizability is determined from the observed dielectric constant  $\epsilon$  using the Clausius-Mossotti relation  $\alpha = (3/4\pi N)(\epsilon - 1)/(\epsilon - 2)$ .  $\alpha_{\text{aniso}}$  depends directly on the local order parameters, the alignment  $\sigma_i(T)$  and the eccentricity  $\eta_i(T)$ , through the relation

$$\alpha_{\text{aniso}} = -\frac{1}{3} \Delta \alpha \left\{ \sigma_i(T) P_2[\cos \Theta_E(i)] + \frac{3}{2} \eta_i \sin^2 \Theta_E(i) \cos[2\Phi_E(i)] \right\}. \quad (2)$$

$[\Theta_E(i), \Phi_E(i)]$  are the polar angles specifying the orientation of the electric field with respect to the local symmetry axes.  $\alpha_{\text{aniso}} = 0$  at high temperatures, but at low temperatures there is a finite contribution depending on the nature of the ordering and the correlations between the order parameters and the local molecular axes. If there are no correlations, the variables  $(\sigma_i, \eta_i)$  and  $[\Theta_E(i), \Phi_E(i)]$  are separable, and one can perform independent averages over the positions and the order parameters. For a powder sample, the average vanishes if the variables are separable. For perfect Pa3 ordering in a single crystal, Meyer and colleagues<sup>26</sup> showed that the average is also zero. This result is very important for the current experiments because the background signal vanishes for the disordered phase and for simple periodic ordering. The measurements are therefore particularly sensitive to the correlations between the order parameters and the configurations of the molecular axes which is exactly what one wishes to study for the glass states. It is important to note that for the trivial low temperature para-dielectric state with molecular axes and order parameters locally frozen, these correlations simply vanish. The correlations provide the key to probing the underlying nature of this class of glasses.

In the experiments reported here, the applied electric fields are used to measure the dielectric susceptibilities and

their thermal history in order to determine the dynamical behavior of the order parameters. The external electric field by itself is not used as a means of generating glass behavior, as it is not the field conjugate to the order parameter. Indirectly, however, because of the coupling between the centers of mass and the orientation of the molecules arising from steric hindrance, there will be a secondary effect where applied electric fields will induce reorientations that can lead to measurable effects in high sensitivity measurements.

Because of the lack of the required experimental sensitivity in the past, no dielectric susceptibility experiments were carried out for N<sub>2</sub>-Ar solid solutions because these molecules do not possess a permanent dipole moment. CO with its small intrinsic dipole moment has been used for the dielectric spectroscopy of orientational glasses but the phase separation of CO-Ar solutions hinders systematic studies of dielectric behavior. However, the dielectric spectroscopy of CO/N<sub>2</sub>/Ar solid solutions<sup>18,29</sup> showed that the CO reorientation rate slowed down through audio frequencies from 15 to below 4 K. From the temperature dependence of the mean CO reorientation rate, Liu *et al.*<sup>18</sup> concluded that cooperative freezing processes are not involved in the slowing of the molecular reorientation rates, but whether this kinetic effect is intimately related to the formation of the quadrupolar glass was not clear. No cusp maxima were observed in dielectric measurements at microwave frequencies for N<sub>2</sub>-Ar mixtures<sup>17</sup> corresponding to the orientational glass state. However, the characteristic reorientational time scale<sup>5</sup> for this glass state is  $10^{-4}$  s, and one would not expect to observe the effects of the glass regime at microwave frequencies. Moreover, the aging behavior observed<sup>8</sup> for pure solid N<sub>2</sub> is seen only in the audio frequency range. With the ability to measure the real part of the dielectric constant with a sensitivity of two parts per billion at audio frequencies,<sup>30</sup> one can probe the local ordering in the quadrupolar glass state in N<sub>2</sub>-Ar mixtures down to 4.2 K and investigate the glass boundary very accurately.

### III. EXPERIMENTAL DATA

As discussed in the preceding section, previous studies had not been able to detect a clear experimental demarcation or phase boundary between the low temperature orientational glass state and the high temperature rotationally disordered phase in solid N<sub>2</sub>-Ar mixtures. In addition, none of the memory or aging effects that characterize glass states had been observed. In contrast, Fig. 2 shows the results of high sensitivity measurements of the dielectric constant of N<sub>2</sub>-Ar mixtures carried out for various N<sub>2</sub> concentrations above 51%. Unmistakable hysteresis effects are observed for thermal cycles in the glass states. In Fig. 2  $\epsilon'$  is the value of  $\epsilon$  at 4.2 K on the lower warm-up curve. The measuring field of 5 kV/m at 1 kHz was turned on at 4.2 K, and for this set of data the sample temperature was never raised above 35 K while the field was on. All the samples were prepared first by mixing the gases at room temperature for more than 24 h and then condensing to the liquid phase at least twice. After each condensation, the complete sample was brought back to room temperature before recondensing, and then finally an-

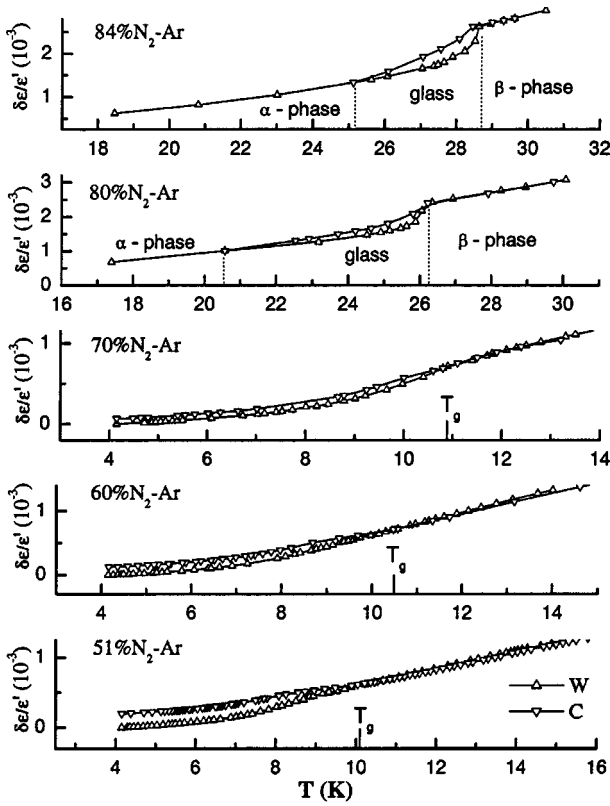


FIG. 2.  $\varepsilon(T)$  of  $N_2$ -Ar mixtures below 30 K for 1 kHz and 5 kV/m measuring field. The field was turned on at 4.2 K and the sample temperature was never raised above 35 K while the field was applied. For 84 and 80 %  $N_2$ -Ar mixtures the hysteresis between the values measured for warming (open triangles) and cooling (inverted open triangles) occurs only in the glass state which is sandwiched between the  $\beta$  and  $\alpha$  phases for these samples. The hysteresis loop increases with decreasing  $N_2$  concentration. For 70, 60, and 51 %  $N_2$ -Ar mixtures, the hysteresis loop is open down to 4.2 K and the onset of the glass regime (indicated by  $T_g$ ) is characterized by the change of slope of  $\varepsilon(T)$ .  $W$  and  $C$  designate warming and cooling cycles respectively. The areas of the hysteresis loops can be related to the glass temperatures through a generalized fluctuation-dissipation relation.

nealed near the solid-liquid transition temperature for 6 to 8 h while monitoring the saturated vapor pressure to check for further gas flow and remove/reduce voids as much as possible. The absolute value of the dielectric constant obtained at 4.2 K from multiple solid samples (for the same gas mixture annealed as explained earlier) clearly showed that additional gas did not enter the cell and similar temperature dependence of  $\varepsilon(T)$  for  $T < 30$  K showed that phase separation of  $N_2$  and Ar did not occur for any of the mixtures studied. To avoid further gas flow, a fine capillary with a heater wound around it in vacuum jacket is used as a sample fill line and once the sample is condensed the heater is turned off to freeze all remaining gas at 4.2 K at a point remote from the neck of the sample cell. For the sample with 90%  $N_2$ , no hysteresis was observed in  $\varepsilon(T)$  with thermal cycling below 35 K, and  $\varepsilon(T)$  changed smoothly without any observable jump at  $T_{\alpha\beta}$  (Fig. 3). A distinct jump is observed only for  $x(N_2) = 100\%$ . For  $x(N_2) < 100\%$ ,  $T_{\alpha\beta}$  is characterized by

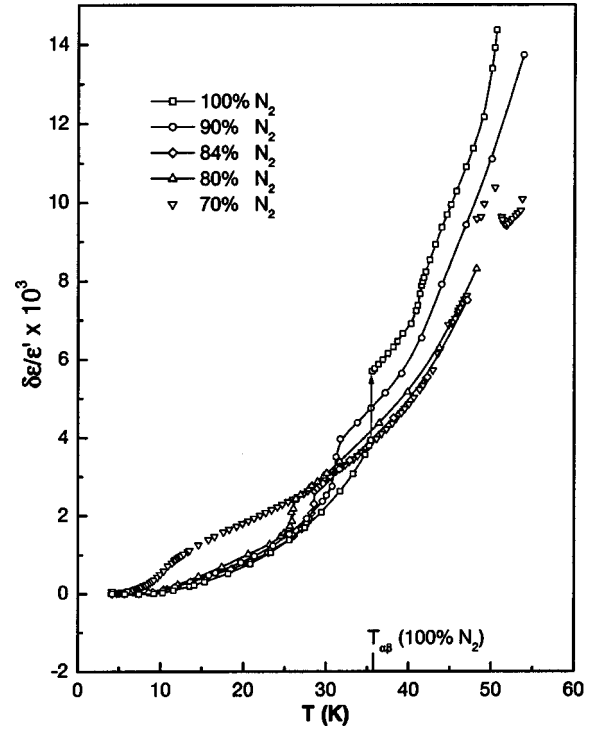


FIG. 3.  $\varepsilon(T)$  of zero field cooled  $N_2$ -Ar mixtures for 1 kHz and 5 kV/m excitation field for  $70 < x(N_2) < 100$  mol%. A distinct jump at the  $\alpha\beta$  transition is clearly seen only for pure  $N_2$ . The values of  $T_{\alpha\beta}$  shift to lower temperatures with decreasing  $N_2$  concentration. Only warming data are shown.

the change of slope in  $\varepsilon(T)$  at this temperature.

### A. Hysteresis effects

For samples with 84%  $N_2$  we observed a strong hysteresis loop in  $\varepsilon(T)$  (Fig. 2), when the sample is thermally cycled between 4.2 and 30 K. The low temperature  $\alpha$  and high temperature  $\beta$  phases are identified at either end of the hysteresis loop. This is the first direct observation of the expected glass behavior in the orientational glass state of  $N_2$ -Ar mixtures. The onset of the hysteresis behavior is very clear for all the samples studied.

Figure 2 shows  $\varepsilon(T)$  for four additional samples with decreasing  $N_2$  concentration. For all the plots in Fig. 2, up triangles represent data taken while warming and down triangles represent data taken while cooling. It is clear from these plots that  $T_g$  progressively decreases with decreasing  $N_2$  concentration. Most significantly, the hysteresis loop in  $\varepsilon(T)$  becomes open ended at 4.2 K for  $x(N_2) < 77\%$ , i.e., there is no transition to the long range orientationally ordered state for  $x(N_2) < 77\%$ . We identify the onset of the glass state with the temperature ( $T_g$ ) for which one observes the closing of the hysteresis loop and the discontinuity in the slope  $d\varepsilon(T)/dT$ . This onset temperature is taken as the transition temperature to the glass state in the phase diagram of Fig. 1. These plots show that the hysteresis increases with decreasing  $N_2$  concentration.

Figure 1 summarizes the results obtained from the study of the detailed dielectric response functions of  $N_2$ -Ar solid



TABLE I. Dependence of the hysteresis area  $\mathcal{H}$  on nitrogen concentration.

$x(\text{N}_2)(\%)$	$T_g(\text{K})$	$\mathcal{H}(\% \text{K})$	$\mathcal{H}/\mathcal{H}_{\text{max}}$	$(\mathcal{H}/\mathcal{H}_{\text{max}})/[1-x(\text{N}_2)]$
84	28.6	0.08	0.036	0.23
80	26.2	0.06	0.027	0.14
70	10.8	0.07	0.032	0.11
60	10.5	0.12	0.054	0.14
51	10.1	0.17	0.077	0.16

solutions. The solid circles designating the transitions from the hcp to the glass state for N<sub>2</sub> concentrations down to 51% are from this work (region IIB). The solid line (and solid squares) mark the separation of the high temperature hcp phase from the high-temperature part of the fcc phase as obtained from x-ray studies.<sup>14</sup> The area covered by the dashed lines represents the region of the orientational glass phase studied by the measurements reported here. We obtained  $35.51 \pm 0.10$  K for the  $\alpha$ - $\beta$  transition temperature  $T_{\alpha\beta}$  compared to the accepted value of 35.61 K. From the observed hysteresis loops as well as from the accuracy of our thermometers, we conclude that the phase boundary between fcc and hcp phases (solid curve separating regions III and IIB) does not coincide with a simple orientational order/disorder transition, but rather that there is an intermediate phase between the disordered  $\beta$  phase and the cubic Pa3 structure. The branching of the lines connecting solid circles for N<sub>2</sub> concentrations greater than 77% shows that an orientational glass regime exists even in the fcc phase. Also from Fig. 1, it is clear that the new phase (region IB) observed by Hamida *et al.*<sup>5</sup> where the mean order parameters evaluated with respect to the local axes have a very narrow distribution (or quadrupolarization), is a part of the orientational glass state identified from these dielectric measurements.

It is instructive to consider the observed hystereses, and their dependence on the argon concentration, using the generalized fluctuation-dissipation relation developed by Cugliandolo and Kurchan.<sup>12,31</sup> The observed areas  $\mathcal{H}[x(\text{N}_2), T_G]$  of the hystereses are listed in Table I for different concentrations, and also shown scaled relative to  $\mathcal{H}_{\text{max}} \sim 2.2 \times 10^{-2}$  K. Cugliandolo and Kurchan considered the off-equilibrium response function  $\mathcal{R}(t, t_w)$  for the order parameter correlation function  $\mathcal{C}(t, t_w)$  observed for spin glasses and related systems at time  $t$  when an applied field is cut off at time  $t_w$ . They developed a generalized relation  $\mathcal{R}(t, t_w) = \beta \int X(\mathcal{C}) d\mathcal{C}$ , where for equilibrium states  $X(\mathcal{C}) = 1$  and  $\mathcal{R}_{\text{eqm}} = \beta D t$ , as expected from the fluctuation-dissipation theorem with  $\beta = 1/(k_B T)$  and  $D$  the diffusion constant. For large  $t$  and  $t_w$ , Cugliandolo and Kurchan<sup>12,31</sup> demonstrated that  $X(\mathcal{C}) \sim T/T_{\text{dyn}}$  where  $T_{\text{dyn}}$  is a characteristic temperature for the onset of glassy dynamics. Summing the expression for  $\mathcal{R}$  over the temperature cycle for the hysteresis, one finds an estimate for the area of the hysteresis given by

$$\mathcal{H} = \sum k_B T \Delta \mathcal{R} \sim (T_G^2/T_{\text{dyn}}) [\mathcal{C}(0, t_w) - \mathcal{C}(t, t_w)]. \quad (3)$$

TABLE II. Concentration dependence of the change in  $\varepsilon$  at the  $\alpha\beta$  transition.

$x(\text{N}_2)$	$(\delta\varepsilon/\varepsilon) \times 10^3$	$T_{\alpha\beta}$	$[(\delta\varepsilon/\varepsilon)x(\text{N}_2)T_{\alpha\beta}] \times 10^6$
100	5.40	35.51	1.5
90	3.96	31.72	1.4
84	2.63	28.63	1.1
80	2.42	26.2	1.2

Making the extrapolation that the hysteresis  $\mathcal{H}$  observed for the dielectric constant in the current experiments, scales in the same fashion as the conjugate field of the order parameters, but must be renormalized to the maximum anisotropy expected for  $\varepsilon$ , we estimate  $\mathcal{H}/\mathcal{H}_{\text{max}} \sim 0.2[1 - Q_{\text{EA}}(t_w)]$ , where  $Q_{\text{EA}}[x(\text{N}_2), t_w]$  is the Edwards-Anderson order parameter for the glass state after the thermal cycle. This result can only be considered as an order of magnitude estimate, but it is in reasonable agreement with the values listed in Table I.

Figure 3 shows the temperature dependence of  $\varepsilon(T)$  observed on warming from low temperatures for zero-field cooled N<sub>2</sub>-Ar mixtures. For the sake of clarity, data for 60 and 51 % N<sub>2</sub> concentrations are not shown in this plot as they are very similar to that of the 70% N<sub>2</sub> sample. The fractional changes in  $\varepsilon$  at the transitions are listed in Table II. The changes decrease with nitrogen concentration and are approximated by

$$\frac{\delta\varepsilon}{\varepsilon} \simeq (1.3 \pm 0.2)x(\text{N}_2)T_{\alpha\beta} \times 10^{-6}. \quad (4)$$

There is no available detailed theory for the observed concentration dependence of the change in  $\varepsilon$  at the transition, but the systematic empirical trend clearly shows that this is an intrinsic property of the transition from the ordered to the disordered state, rather than one induced by random and irreproducible crystalline defects. Note that the general features for the hysteresis and memory effects as summarized in Tables I and II are observed for different samples prepared from different condensations but for the same N<sub>2</sub> concentrations. In the following sections we discuss the dependence of the dielectric response of N<sub>2</sub>-Ar mixtures on the external (ac) electric field.

### B. Electric field dependent behavior in the glass state

In addition to the above results, the results of previous studies<sup>8-10</sup> showed dramatic aging effects as a function of the applied ac electric fields and the thermal history of the sample. Figure 4 shows the dielectric response of a 70% N<sub>2</sub>-Ar sample, first cooled to 4.2 K in zero field, then warmed up to 54 K in 5 kV/m and 1 kHz excitation fields. The sample was annealed during warmup as described in the caption of Fig. 4 in the presence of the field, cooled to 4.2 K (“field cooled”), and then warmed up again. The field induced change of almost 1% in  $\varepsilon(T)$  for  $T < 10$  K, and pronounced hysteretic behavior show that the applied electric field significantly modifies the free energy landscape of com-

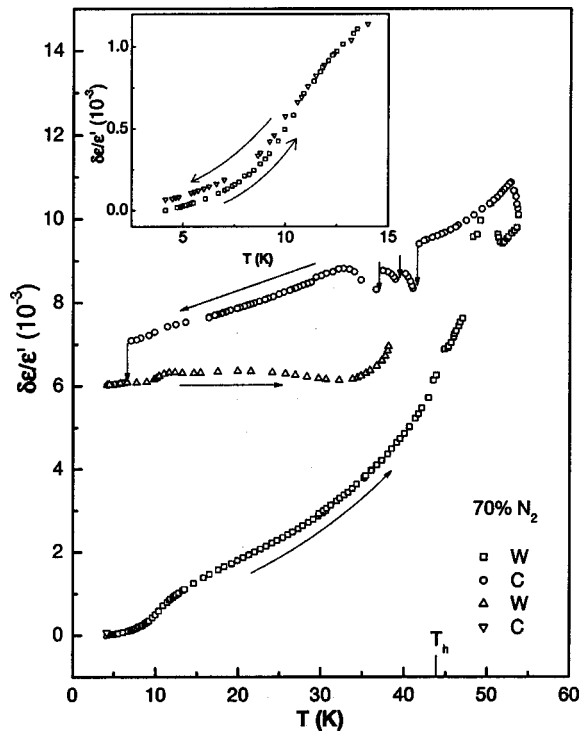


FIG. 4.  $\varepsilon(T)$  of 70%  $N_2$ -Ar mixtures field cooled in 1 kHz and 5 kV/m electric field. Vertical arrows mark the spontaneous changes of polarization at various random temperatures, while arrows along the curves indicate the direction of change in temperature. A kink at  $\sim 44$  K is observed during the first warming cycle, which is produced after annealing at  $42 < T < 45$  K for 6 to 8 h. The sharp increase at  $T \sim 49$  K on annealing is similar to that reported for 100%  $N_2$  (Ref. 8). W and C designate warming and cooling cycles respectively.

plex potential energy minima. In addition, a few sharp drops in the value of  $\varepsilon$  are observed on cooling (but *not* on warming). These appear to be sharp transitions between neighboring configurational minima. The lack of such events on warming implies an effective erasure of memory effects on warming following aging at low temperatures analogous to the phenomena observed in spin-glass systems and consistent with recent views of glass formation in terms of replica symmetry breaking.<sup>12,31</sup> Similar measurements carried out on solid solutions with  $x(N_2)$  of 90, 84, and 80 % showed similar behavior as well (not shown here).

It turns out that in all field cooled measurements, for the sample in Fig. 4 as well as pure  $N_2$  and for all  $N_2$ -Ar samples studied down to 51%  $N_2$  concentration, there exists a characteristic temperature  $T_h$ , such that only samples raised to a temperature  $T > T_h$  in the presence of the field and then cooled shows hysteresis similar to Fig. 4. This hysteresis is erased and the sample retraces the lower curve in Fig. 4 if the sample is annealed at a temperature  $T > T_h$  in zero field for 10 to 12 h and then cooled to 4.2 K. This result shows that the resulting hysteresis is not due to simple volume effects such as annealing of voids, grain boundaries, or new material entering the sample cell. Samples warmed to  $T < T_h$  do not show any hysteresis except in the orientational glass regime;

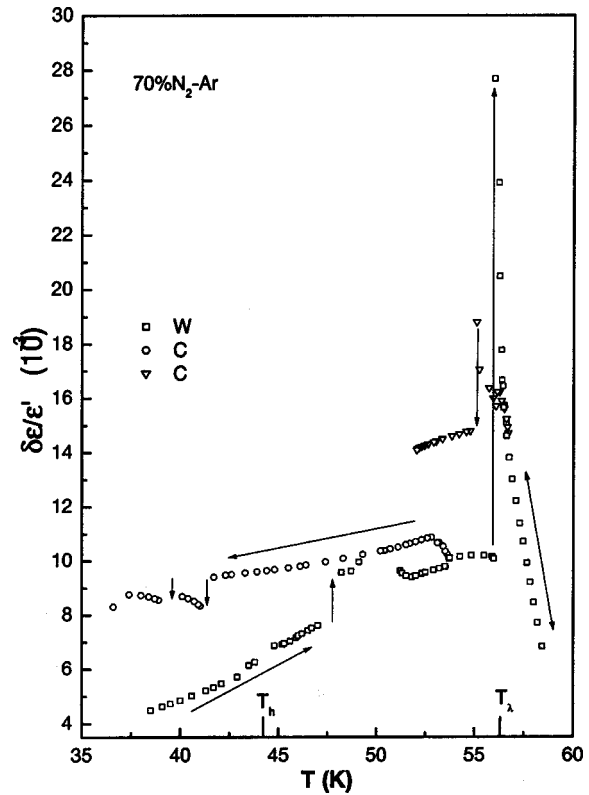


FIG. 5.  $\varepsilon(T)$  of 70%  $N_2$ -Ar mixtures field cooled in 1 kHz and 5 kV/m electric field near melting temperature. A sharp peak in the temperature dependence for  $\varepsilon(T)$  as well as small hysteresis occurs at  $T_\lambda$ . The bidirectional arrow indicates a region with no hysteresis and vertical arrows indicate spontaneous change of  $\varepsilon(T)$ . W and C designate warming and cooling cycles, respectively.

e.g., for a sample raised to 15 K only, the results shown in the inset of Fig. 4 are similar to the zero field results of Fig. 2.

Figure 5 shows the data for 70%  $N_2$ -Ar mixture raised to 58 K in the presence of the field. A  $\lambda$ -like cusp behavior was observed at  $T_\lambda = 56.5$  K which is distinct from the  $\alpha\beta$  lattice transition. Above  $T_\lambda$ ,  $\varepsilon(T)$  is highly reproducible without any detectable hysteresis as expected for the disordered state. On field cooling below  $T_\lambda$ , another sharp peak is observed at  $T = T_\lambda - 1.0$  K with reduced peak height. When compared with the cusp maxima observed for  $\varepsilon$  for a 100%  $N_2$  at  $T_\lambda$ ,<sup>8</sup> the peak height for 70%  $N_2$  sample is about 1.75 times smaller; i.e., with decreasing  $N_2$  concentration the cusp maxima decreases. As pointed out earlier, these results do not indicate a phase separation of  $N_2$  and Ar.

For 60%  $N_2$ -Ar samples, a strong hysteresis is observed similar to the 70%  $N_2$ -Ar samples, but the characteristic spontaneous jumps in  $\varepsilon(T)$  are missing, as shown in Fig. 6. This indicates that samples with decreasing concentrations of  $N_2$  show decreasing sharp features. The cusp feature at  $T_\lambda$  is further reduced in amplitude by a factor of 3.5. Above 57 K,  $\varepsilon(T)$  varies linearly with increasing temperature up to the melting temperature ( $T_M$ ), where a sharp drop occurs (Fig. 7). For  $T > T_\lambda$ ,  $\varepsilon(T)$  is highly reproducible without hysteresis. Similar to the 60%  $N_2$  sample,  $\varepsilon$  for a 51%  $N_2$ -Ar sample in Fig. 8 shows a sharp increase at  $T_\lambda - 1.2$  K. At

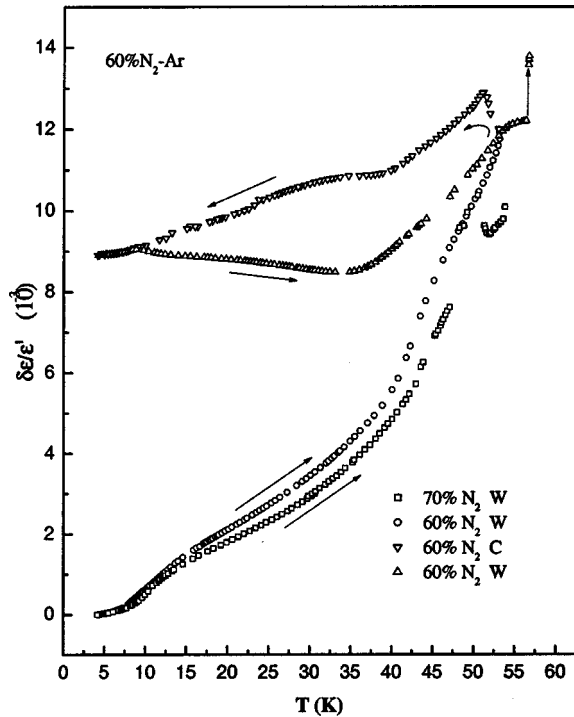


FIG. 6.  $\epsilon(T)$  of 60% N<sub>2</sub>-Ar mixtures field cooled in 1 kHz and 5 kV/m electric field. Although no spontaneous changes in polarization are observed, strong field-induced hysteresis is observed. Also no kink at  $\sim 44$  K is observed but there exists a change of slope at this temperature. Arrows indicate the direction of change in temperature while W and C designate warming and cooling cycles, respectively.

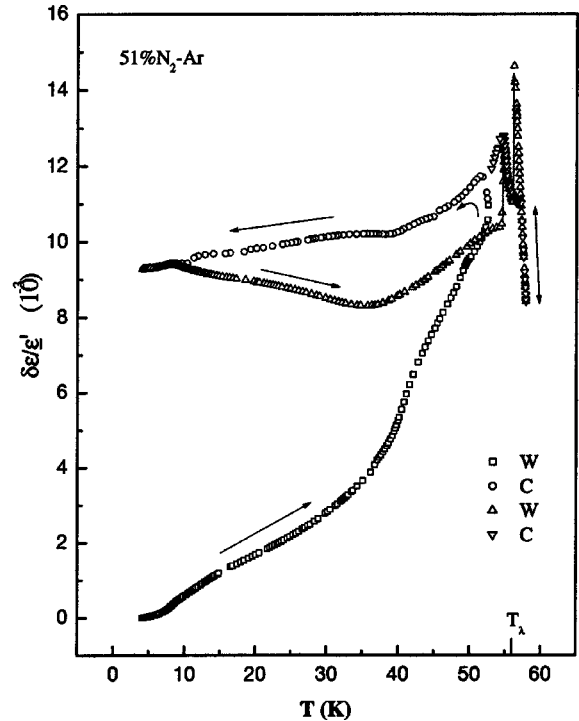


FIG. 8.  $\epsilon(T)$  of 51% N<sub>2</sub>-Ar mixtures field cooled in 1 kHz and 5 kV/m electric field. No kink at  $\sim 44$  K is observed but the change of slope about this temperature is observed. A  $\lambda$ -like cusp in  $\epsilon(T)$  is observed at  $T_\lambda$ , as well as a smaller peak in  $\epsilon(T)$  below  $T_\lambda$ . Arrows indicate the direction of change in temperature while W and C designate warming and cooling cycles, respectively.

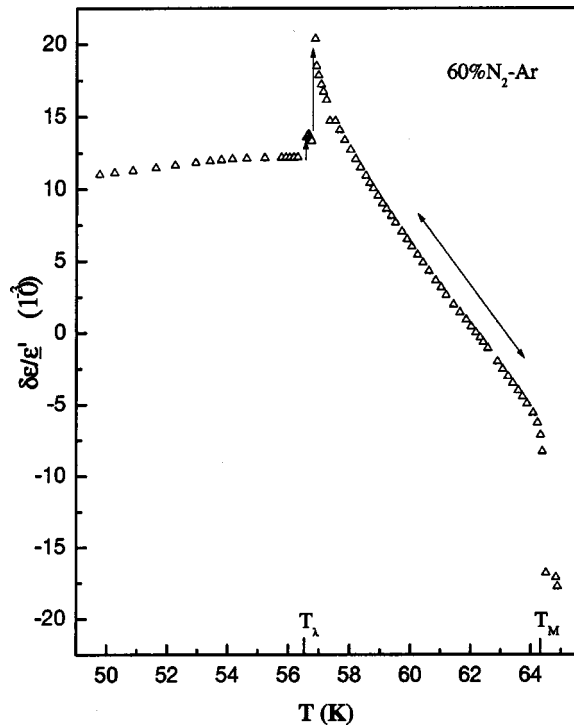


FIG. 7.  $\epsilon(T)$  of 60% N<sub>2</sub>-Ar mixtures field cooled in 1 kHz and 5 kV/m electric field near melting temperature. A  $\lambda$ -like cusp in  $\epsilon(T)$  at  $T_\lambda$  as well as a smaller peak in  $\epsilon(T)$  below  $T_\lambda$  is observed. Bidirectional arrow indicates region with no hysteresis while vertical arrows show rapid change in  $\epsilon(T)$  in time.

$T_\lambda$ , the cusp maximum is reduced by a factor of 7. For  $T > T_\lambda$ , no hysteresis is observed in  $\epsilon$  for any of the samples studied, indicating that the solid is in a “rotational-melt” state; i.e., for  $T_\lambda < T < T_M$ , the individual molecules are completely free to rotate before the lattice meltdown at  $T_M$ .

Our observations indicate that below  $T_h$ , for zero field cooled samples of all N<sub>2</sub>-Ar mixtures,  $\epsilon(T)$  attains equilibrium value very quickly (typically in a few sec) when  $T$  is changed, but for field cooled samples the time required to attain equilibrium value varies from few minutes to few hours depending on the temperature. In particular, for  $41.5 < T < 43$  K,  $\epsilon(T)$  changes slowly in 6 to 8 h resulting in a kink at  $T_h$  and for  $50 < T < 53$  K it changes in 10 to 12 h resulting in a peak at 52 K. For  $T < 41$  K as well as for  $53 < T < 56$  K,  $\epsilon(T)$  attains equilibrium value in a few minutes but for  $T > 56$  K the response is similar to the zero field cooled samples (i.e., a few sec).

#### IV. CONCLUSION

The results reported here for high sensitivity measurements of the dielectric susceptibility of solid N<sub>2</sub>-Ar mixtures have provided new information about the nature of the phase diagram for the orientational degrees of freedom of molecular rotors in the presence of disorder. Distinct hysteresis effects have been observed and these are attributed to the onset of the glassy dynamics and memory phenomena of the quadrupolar glass states previously inferred from NMR studies.

Exploration of the temperature dependence of the dielectric constant on thermal cycling, with and without applied electric fields, have revealed the existence of history-dependent nonequilibrium behaviors for the electric response function. The areas of the hystereses measured for thermal cycles for a series of samples with different concentrations, were observed to increase systematically with increasing disorder (increasing Ar concentration). The order of magnitude of the observed hystereses is consistent with the values estimated from the generalized off-equilibrium response function as developed for glass systems by Cugliandolo and Kurchan.<sup>12,31</sup>

The glasslike behavior in this class of systems is attributed to the combined effects of strong geometrical frustration and the substitutional disorder which leads to a thermodynamically large number of almost degenerate ground states. Applied ac electric fields in the range 1–10<sup>3</sup> kHz are effective in perturbing this energy landscape, resulting in the observed field-cooling effects similar to (but not identical to) those observed in frustrated magnetic systems. It is important to note that the ac electric field is not the conjugate field to the order parameters for molecular rotators (which would be an electric field gradient) but the polarization induced by the field can nevertheless induce changes in the molecular orientations that depend on the local geometrical correlations [Eq.

(2)]. These effects are erased on warming to a well-defined temperature region. We do not believe that the observations are attributable to static brute force effects of the applied field. We rather believe that the applied fields can significantly alter the dynamics of the approach to thermal equilibrium. With energies of the order of  $E_{\text{field}} = 10^{-22}$  ergs/molecule, the applied fields will lift by small amounts the degeneracies in energies of some cluster configurations. If these changes in energy are comparable to or greater than the width of the energy states, the transition rates become altered quite significantly. This would be observed for transition frequencies  $\omega \sim E/\hbar \sim$  kHz which is consistent with the results presented here.

The onset of the hysteresis observed for  $\epsilon(T)$  provides much clearer evidence for a transition to the glass state for solid N<sub>2</sub>-Ar mixtures than previously obtained by NMR. The results also provide corroborating evidence for the existence of local ordering in a glass state in the low-N<sub>2</sub> fcc phase where the field effects become less pronounced with decreasing N<sub>2</sub> concentration. While it is clear from the results reported that glass behavior with pronounced memory effects do occur in this system and with magnitudes in good qualitative agreement with extended fluctuation-dissipation arguments, we emphasize that this report is empirical and that a deeper theoretical understanding remains to be developed.

\*Present address: Department of Physics, University of California, San Diego, CA 92093.

Electronic address: manyam@physics.ucsd.edu

<sup>1</sup>K. Binder and J. D. Reger, *Adv. Phys.* **41**, 547 (1992).

<sup>2</sup>A. P. Ramirez, *Annu. Rev. Mater. Sci.* **24**, 453 (1994).

<sup>3</sup>M. J. P. Gingras, C. V. Stager, N. P. Raju, B. D. Gaulin, and J. E. Greedan, *Phys. Rev. Lett.* **78**, 947 (1997).

<sup>4</sup>T. A. Scott, *Phys. Rep.* **27**, 89 (1976).

<sup>5</sup>J. A. Hamida, N. S. Sullivan, and M. D. Evans, *Phys. Rev. Lett.* **73**, 2720 (1994).

<sup>6</sup>J. A. Hamida, E. B. Genio, and N. S. Sullivan, *J. Low Temp. Phys.* **103**, 49 (1996).

<sup>7</sup>M. H. Muser and P. Nielaba, *Phys. Rev. B* **52**, 7201 (1995).

<sup>8</sup>S. Pilla, J. A. Hamida, and N. S. Sullivan, *New J. Phys.* **3**, 17.1 (2001).

<sup>9</sup>S. Pilla, J. A. Hamida, K. A. Muttalib, and N. S. Sullivan, *Phys. Lett. A* **256**, 75 (1999).

<sup>10</sup>S. Pilla, J. A. Hamida, K. A. Muttalib, and N. S. Sullivan, *Physica B* **284–288**, 1125 (2000).

<sup>11</sup>H. Meyer, *Physica B* **197**, 13 (1994).

<sup>12</sup>L. F. Cugliandolo and J. Kurchan, *Phys. Rev. Lett.* **71**, 1 (1993).

<sup>13</sup>K. Jonason, E. Vincent, J. Hammann, J. P. Bouchaud, and P. Nordblad, *Phys. Rev. Lett.* **81**, 3243 (1998).

<sup>14</sup>C. S. Barrett and L. Meyers, *J. Chem. Phys.* **42**, 107 (1965).

<sup>15</sup>J. A. Hamida, S. Pilla, and N. S. Sullivan, *J. Low Temp. Phys.* **111**, 365 (1998).

<sup>16</sup>D. Esteve, N. S. Sullivan, and M. Devoret, *J. Phys. (Paris), Lett.* **43**, 793 (1982).

<sup>17</sup>W. Kempinski and J. Stankowski, *Low Temp. Phys.* **21**, 74 (1995).

<sup>18</sup>Shang-Bin Liu and M. S. Conradi, *Solid State Commun.* **49**, 177 (1984).

<sup>19</sup>L. G. Ward, A. M. Saleh, and D. G. Haase, *Phys. Rev. B* **7**, 1832 (1983).

<sup>20</sup>W. Press, B. Janik, and H. Grimm, *Z. Phys. B: Condens. Matter* **49**, 9 (1982).

<sup>21</sup>U. T. Höchli, K. Knorr, and A. Loidl, *Adv. Phys.* **39**, 405 (1990).

<sup>22</sup>K. H. Michel and J. M. Rowe, *Phys. Rev. B* **22**, 1417 (1988).

<sup>23</sup>P. Wochner, E. Burkel, J. Peik, and A. Eckold, *Europhys. Lett.* **17**, 703 (1992).

<sup>24</sup>N. S. Sullivan, *Can. J. Chem.* **66**, 908 (1988).

<sup>25</sup>H. Klee, H. O. Carmesin, and K. Knorr, *Phys. Rev. Lett.* **61**, 1855 (1988).

<sup>26</sup>B. A. Wallace, Jr. and H. Meyer, *J. Low Temp. Phys.* **15**, 297 (1974).

<sup>27</sup>J. H. Constable, C. F. Clark, and J. R. Gaines, *J. Low Temp. Phys.* **21**, 599 (1975).

<sup>28</sup>G. Marsoulis and D. M. Bishop, *Mol. Phys.* **58**, 271 (1986).

<sup>29</sup>Shang-Bin Liu and M. S. Conradi, *J. Chem. Phys.* **78**, 6901 (1983).

<sup>30</sup>S. Pilla, J. A. Hamida, and N. S. Sullivan, *Rev. Sci. Instrum.* **70**, 4055 (1999).

<sup>31</sup>G. Parisi, *Nuovo Cimento D* **20**, 2021 (1998).